PERGAMON

Journal of Structural Geology 23 (2001) 873–885

JOURNAL OF STRUCTURAL GEOLOGY

www.elsevier.nl/locate/jstrugeo

Development of crystal morphology during unitaxial growth in a progressively widening vein: II. Numerical simulations of the evolution of antitaxial fibrous veins

C. Hilgers[a,*], D. Koehn[b], P.D. Bons[b,c], J.L. Urai[a]

[a]*Geologie—Endogene Dynamik, RWTH Aachen, D-52056 Aachen, Germany*
[b]*Tektonophysik—Institut für Geowissenschaften, Universität Mainz, D-55099 Mainz, Germany*
[c]*Earth Processes Simulation Laboratory, Department of Earth Sciences, Monash University, Clayton (Melbourne), VIC 3168, Australia*

Received 12 January 1999; accepted 23 November 1999

Abstract

The development of fibrous morphology and capability of fibres for tracking the opening trajectory were investigated using numerical simulations of a natural antitaxial fibrous vein. Starting from a non-unique best case, variation of fracture opening velocity, grain size, wall roughness, growth anisotropy and crystal growth velocity shows that these parameters differ in importance for crystal morphology and tracking capability. Fibrous veins can be simulated using crack–seal opening of the fracture. Grain boundaries track the opening trajectory if the wall roughness is high, opening increments are small and crystals touch the wall before the next crack increment starts.

1. Introduction

The crystal morphology of many syntectonic veins cannot be explained by classical crystal growth theories (Tang et al., 1990; Thijssen et al., 1992; Bennema, 1996). Often the observed microstructure is not the one produced by free growth of faceted polycrystals from a supersaturated solution, where anisotropic growth velocities result in a 'blocky' texture due to growth competition. Rather, elongate-blocky to fibrous morphologies are observed, often containing curved crystals without the corresponding lattice curvature (Urai et al., 1991; Fisher and Brantley, 1992; Crespi and Chan, 1996; Bons and Jessell, 1997; Means and Li, 2001, this issue). These unusual microstructures have been long known (Taber, 1918 and references therein) and Mügge (1928) explained their formation by proposing crystal growth which keeps track with syntectonic opening. This mechanism provides an external boundary condition which suppresses the growth competition and allows growth of all original crystals.

Durney and Ramsay (1973) proposed that syntectonic fibres grow along the opening trajectory. Although the kinematics of crystal growth were not explained, the transport mechanism was thought to be a process of diffusional transport into the dilation sites. This process was proposed to be continuous, without the formation of significant fluid-filled openings. Fibrous microstructures quickly became important tools in the analysis of progressive deformation (Ramsay and Huber, 1983, 1987; Spencer, 1991).

Although it is difficult to prove the assumption of tracking in field studies, tests of its validity can be made, for example by checking if the fibres connect corresponding markers. This is an important test, because it has been shown that fibres do not track the opening trajectory in all cases (Cox, 1987; Williams and Urai, 1989; Urai et al., 1991). However, it is rarely carried out in field-based studies.

As an alternative to diffusional, continuous accretion, Ramsay (1980) proposed the discontinuous crack–seal mechanism, a repeated process of cracking and sealing, as indicated by the characteristic inclusion bands/trails and stair-stepped grain boundaries. The distance between two inclusion bands/-trails, assumed to represent individual crack increments, is usually in the range of 2–30 μm (Cox, 1987; Fisher et al., 1995).

In recent papers (Fisher and Brantley, 1992; Bons and Jessell, 1997) it was suggested that fibres could only form by a diffusional accretion process, based on experiments and theoretical modelling.

Kinematic models to explain the fibrous morphologies were presented by Cox and Etheridge (1983) and Urai et al. (1991). Based on these models, simulations of natural

* Corresponding author. Fax: +49-241-888-8358.
E-mail address: c.hilgers@ged.rwth-aachen.de (C. Hilgers).

0191-8141/01/$ - see front matter
PII: S0191-8141(00)00160-7

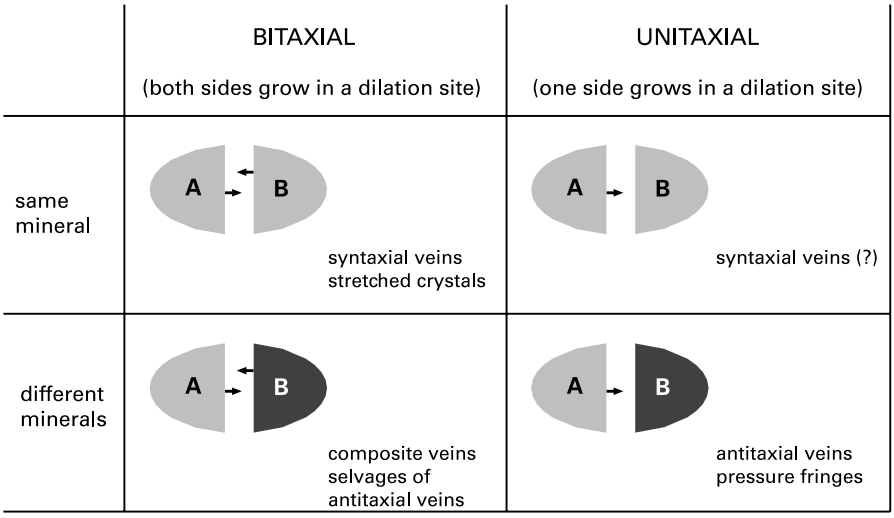

Fig. 1. Schematic illustration of the four different configurations for crystal growth in a single dilation site. Width of the site is unspecified, the range relevant for this study is between a few nm (the width of a grain boundary) and 1 mm. Note that this new classification considers a much smaller scale than the ones traditionally used. For each of the four combinations the corresponding larger scale microstructure is indicated.

microstructures were carried out by Hilgers et al. (1997). More recently, a computer programme (Bons, 2001, this issue) has made such simulations much less time consuming.

When considering the basic processes of accretion in a dilation site, the growth can be either *unitaxial* or *bitaxial*, as shown in Fig. 1. We introduce the terms unitaxial and bitaxial (at the risk of creating more confusion than clarification), to show how these four basic cases are responsible for all the microstructures observed, and to show the link with the general definition of mobile grain boundaries (Urai et al., 1986, p. 166).

This study addresses the unitaxial case described above. It aims at testing the kinematic models of Urai et al. (1991) and Bons (1997) against observations of natural antitaxial fibrous veins. First, we attempt to simulate the observed microstructures using reasonable input parameters to get a 'best case' model. Secondly, we present a sensitivity analysis of the best case model, by varying the input parameters to see how the correspondence with observations changes.

2. Microstructural observations

Because the shape of the wall–vein interface is a critical parameter, selected samples were studied in detail. Fig. 2 shows samples from localities with sandstone–slate multilayers containing fibrous antitaxial calcite veins. The first sample was taken at Stop 5 of the Paul Williams Conference excursion (Simony, 1998) from the Palaeozoic McKey Group. The second is from the same outcrop in New York State as described in Passchier and Urai (1988) and Urai et al. (1991) and the third was taken from the Tertiary flysch of the Morcles nappe, Switzerland (Durney, 1972; Ramsay et al., 1982, p. 35).

In all three samples, curved but undeformed calcite fibres are concentrated in the shaly part of the multilayer and abut on the calcite-rich sandstone layers. Samples were cut to contain the whole fibre which is continuous across the vein, and were examined by optical microscopy of ultrathin sections and SEM. For SEM studies samples were polished with grinding powder up to 1200 grit and etched with 5% HCl for about 15 s, exposing the calcite grain boundaries and the shape of the wall. In all three samples, calcite grain boundaries are preferentially located at the antiformal peaks of the wall rock irregularities. The crystal width varies depending on the wall rock roughness, but is approximately constant along the crystal long axis with a resulting fibrous morphology. The crystal width in Fig. 2(b) widens towards the less rough fracture wall on the left-hand side. Wall rock fragments are located in the vein centre (Fig. 2c), or near the wall (Fig. 2b). Single mica inclusions in the vein are located either within the calcite crystals or on the grain boundary (Fig. 2b, c). The wall morphologies of both sides do not match with each other (Fig. 2b, c), with antiformal peaks parallel to the local orientation of calcite grain boundaries (Fig. 2a and lower right of Fig. 2c).

Examination with the microscope shows no apparent crystallographic preferred orientation of the calcite. More detailed U-stage studies of fibre orientations are in progress. Veins b and c are surrounded by a quartz-rich selvage which has overgrown the matrix.

3. Simulations

3.1. Procedure of simulation

Simulations were run with the computer programme Vein Growth 2.0 (Bons, 2001). It relaxes some of the constraints

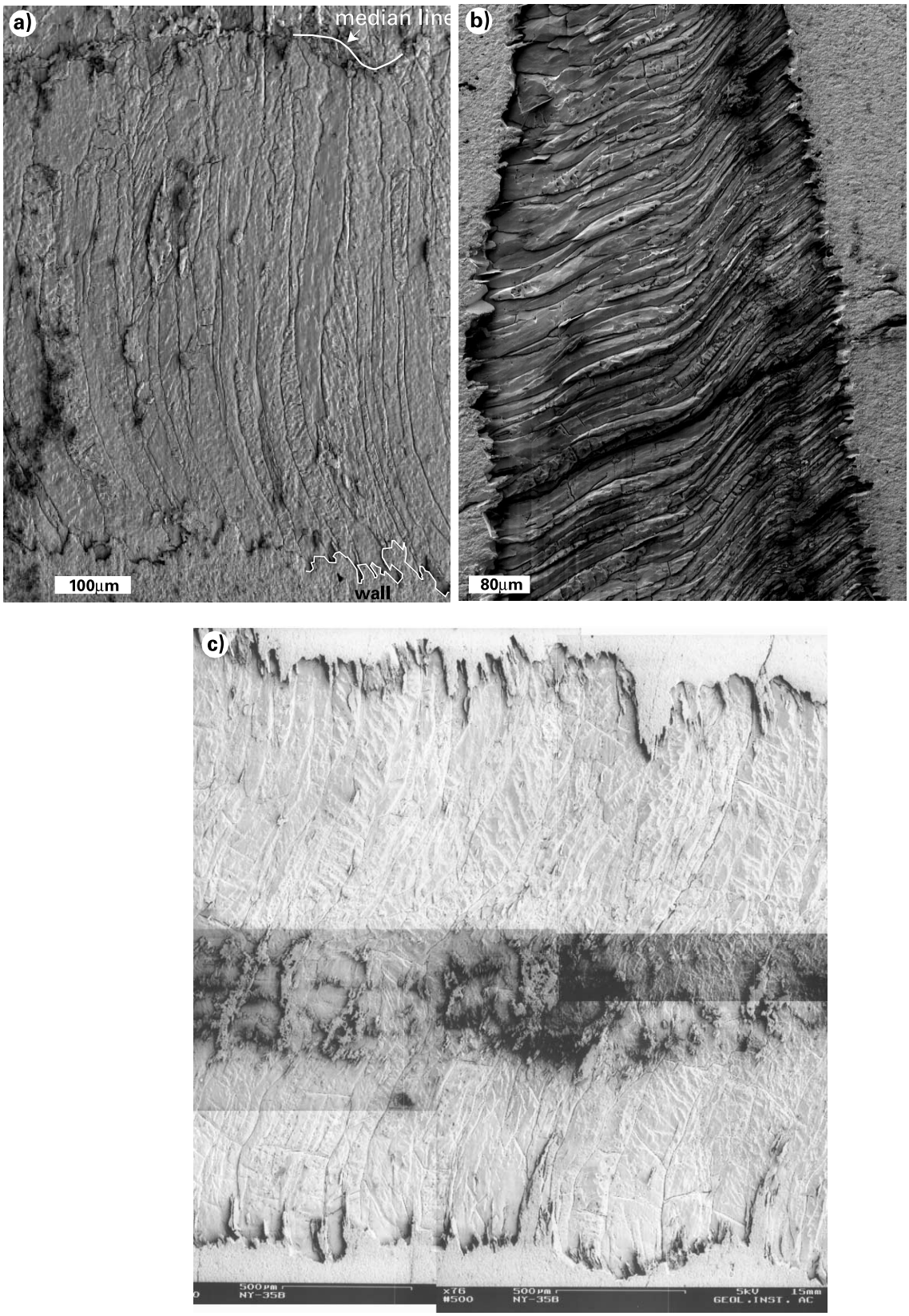

Fig. 2. SEM images of antitaxial calcite fibres in slates from the Canadian Rockies (a), the Morcles nappe, Switzerland (b) and New York State (c). In all samples grain boundaries are located at antiformal peaks of the wall. The crystal width is directly dependent on the wavelength of the wall irregularities.

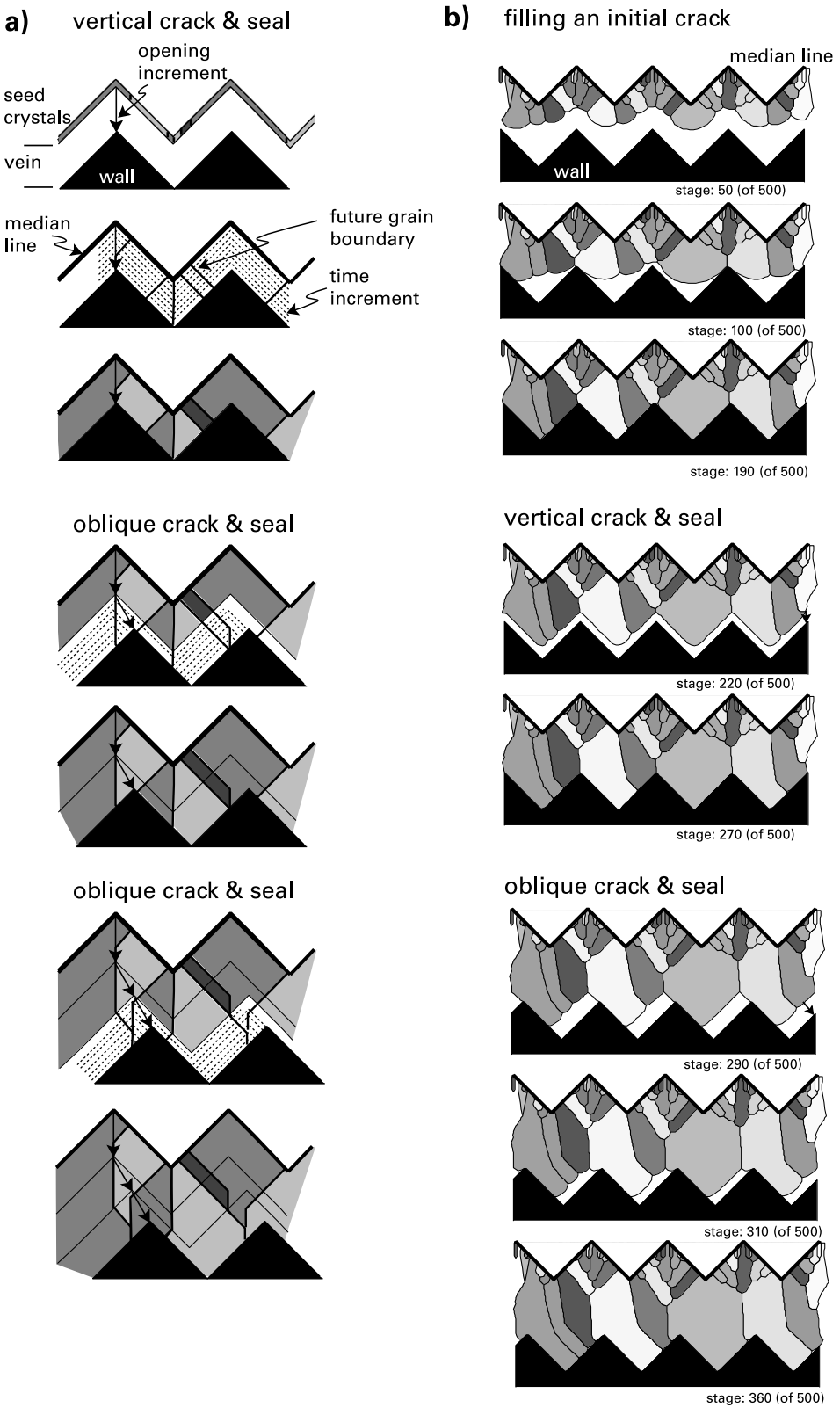

Fig. 3. (a) The kinematic model of Urai et al. (1991) with strictly isotropic growth forces the grain boundaries near the peak to move away at final growth increments during oblique opening. This is the case when the fluid filled space around the wall is of different thickness. (b) Computer simulation of isotropic crystals growing towards the triangular wall. Grain boundaries move towards the antiformal peak of the wall. During oblique opening, all grain boundaries are oriented normal to the wall.

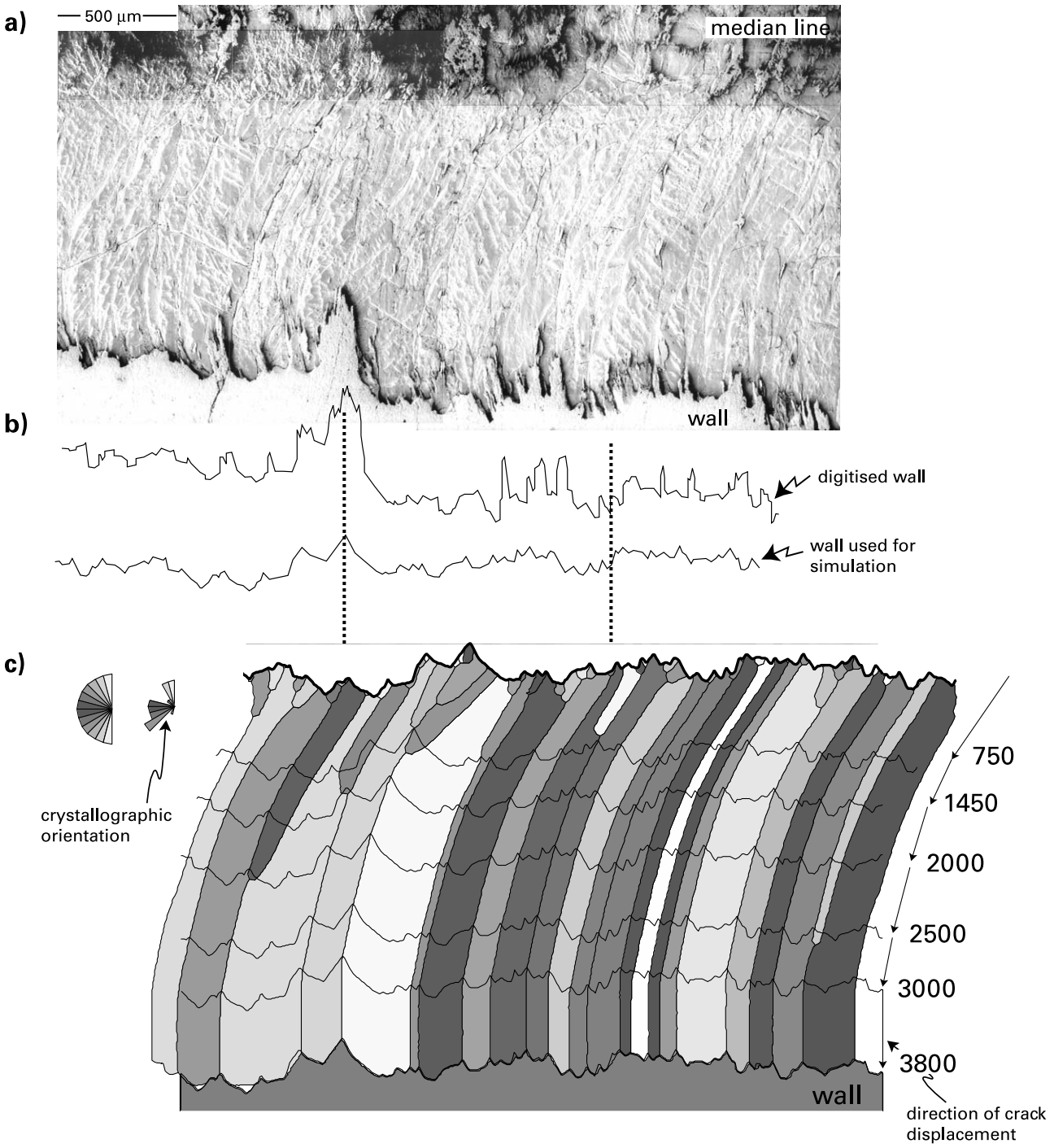

Fig. 4. (a) Half of natural antitaxial fibrous vein from median line to wall (upper half of Fig. 2c). (b) The digitised natural wall was modified in order to allow oblique opening. (c) 'Best case' simulation of natural vein, using the smoothened wall as input parameter. The shaded half circle and the rose diagram at the upper left show the initial random and final orientation of crystallographic axes. Numbers on the arrows on the right indicate the time increment when the opening direction was changed.

of the kinematic model of Urai et al. (1991) and allows two-dimensional simulations of both isotropic and anisotropic crystal growth, using different wall morphologies and initial grain sizes as input parameters.

The kinematic models used in this study have to meet the Mügge (1928) requirement (growth velocity of the slowest growing faces in the vein is larger or equal to the average crack opening velocity). The key process responsible for controlling the microstructural evolution is the movement of vein grain boundaries towards antiformal peaks in the wall (cf. figs. 5 and 6 in Urai et al. (1991)). This occurs because the growing crystals are (semi-continuously or in

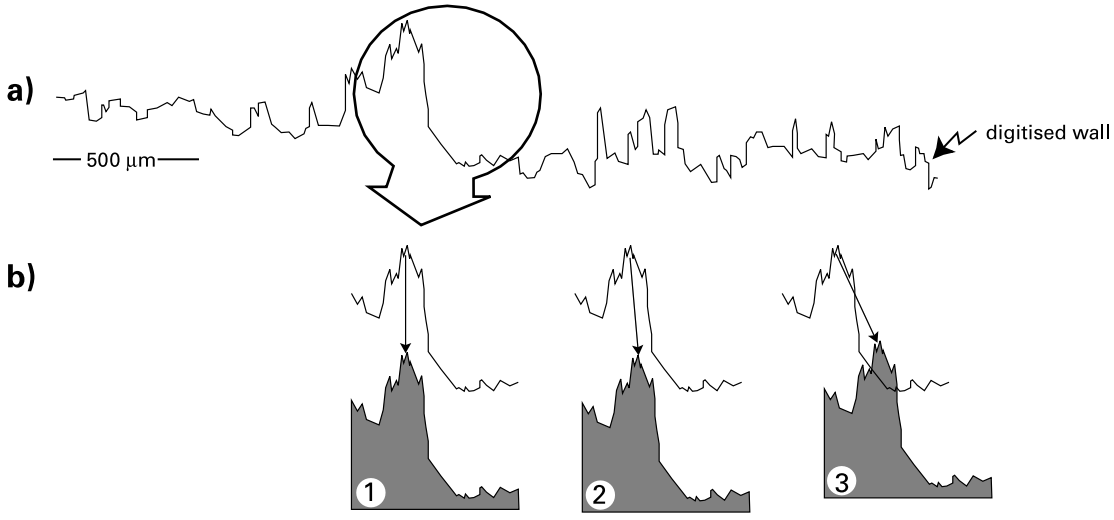

Fig. 5. (a) Sketch illustrates digitised natural wall. (b) The possible variation in orientation of the opening vector without wall rock break-off is limited by the inclination of the wall around the peak (1, 2). If the displacement direction vector crosses the wall, wall rock break-off occurs, which cannot be simulated with our model (3).

frequent intervals) forced to assume the shape of the wall, and subsequent growth starts by the propagation of this irrational surface. We propose to call such peaks in the wall grain boundary attractors (GBAs). Besides attracting the grain boundaries, GBAs have an additional important role: they enhance the growth competition process by attracting several grain boundaries towards one peak. This growth competition process is however fundamentally different from the one controlled by crystallographic orientation during growth of faceted polycrystals (cf. fig. 2b of Cox and Etheridge, 1983).

Although the resulting microstructures are similar, there is an important difference between the models of Urai et al. (1991) and Bons (1997). In the Urai et al. model, growth is strictly isotropic, i.e. the surface of the polycrystal everywhere grows with the same velocity in every direction. A consequence of this model is that grain boundaries rarely reach the peak of a wall irregularity, because the final stages of sealing the crack after oblique opening force grain boundaries away from the peak (Fig. 3a). The Bons (2001) model allows the growing polycrystal to develop grooves where grain boundaries reach the growing interface, in effect mimicking the effect of grain boundary energy during polycrystal growth. This process is illustrated in Fig. 3(b). Interestingly, the effectiveness of GBAs is increased in comparison with the Urai et al. (1991) simulations, because grain boundaries in this case can reach the antiformal peaks in the wall.

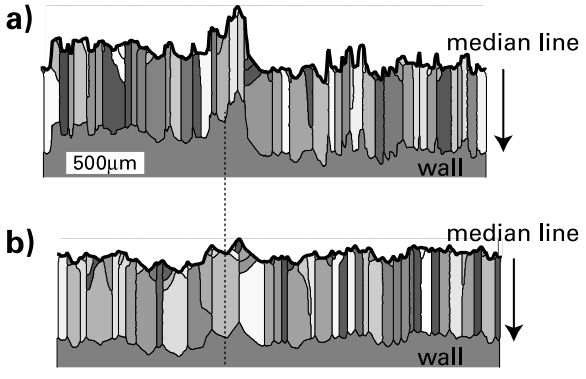

Fig. 6. Computer simulation with opening normal to the wall. Crystal growth from the median line towards the wall fills the vein completely before the next crack increment occurs. (a) The digitised wall from the natural vein shows that grain boundaries are located at marked antiformal peaks of the wall. (b) Similar results were obtained from simulations with the smoothened wall, although minor differences exist in crystal width. Generally more grains survive in (a), as is visible on the left-hand side.

3.2. 'Best case' simulation

First we attempted to find combinations of the input parameters which produce a resemblance as close as possible to that of a natural vein. From a sample from the New York slates (upper half of Fig. 2c), we used the digitised wall morphology (800 x,y values) and the opening trajectory based on grain boundary curvature as input. We then varied the initial grain size, growth velocity, growth anisotropy, and magnitude of opening increments, to arrive at the 'best case' simulation shown in Fig. 4.

The programme assumes that the wall is inert and can neither deform while crystals grow nor incorporate broken-off wall rock fragments into the vein. Vein growth takes place by instantaneous opening a predefined crack with a user-defined width, followed by propagation of the polycrystal's surface. One of the surprises after SEM examination of both the Canadian and the New York State samples (Fig. 2a, c) was that the oblique opening during early stages of growth (as suggested by the fibres) could not have occurred with the presently observed wall as a

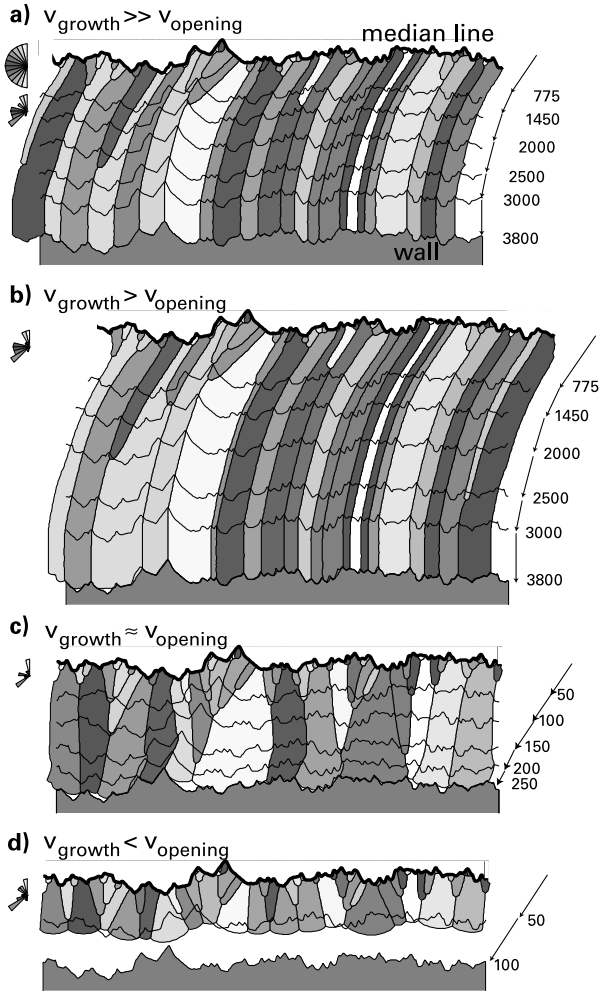

Fig. 7. Simulations of the different opening velocities. While increasing the opening velocity of the fracture, the grains lose contact with the wall and grain boundaries stop tracking the opening trajectory. Within the vein the wall morphology represents its location, when the opening direction is changed. (a) Growth velocity ⩾ opening velocity. Fewer opening events during growth lead to a smaller vein. Grain boundaries track the opening trajectory, because they reach the wall before the next crack increment starts. (b) Growth velocity > opening velocity. 'Best case' simulation from Fig. 4(c) with grain boundaries tracking the opening trajectory. Crystals still seal the fracture before the next crack increment starts. (c) Growth velocity ≈ opening velocity. Grains start to lose contact with the wall, but parts of the grain boundaries track the opening direction (see grain boundary at highest peak of wall). Grains become elongate-blocky without constant width along the grain length axis. Partial sealing of the vein results in partial tracking of the grain boundaries. (d) Growth velocity < opening velocity. New cracks occur, before the grains can seal the fracture. Grain boundaries do not track the opening trajectory and grains are not fibrous.

'template'. Opening the wall–vein interface in its present shape is only possible parallel to the fibres present at the outside of the vein. Oblique opening would result in interlocking (like in a jigsaw puzzle) and break-off of many of the larger irregularities (Fig. 5).

We propose that this is due to a change in shape of the wall during opening, which may be common in nature (see Section 4). To allow the simulations, we reduced the amplitude of the large irregularities as far as to allow for oblique opening. This can be seen as our best guess of the shape of the wall early in the vein's life (Fig. 4b). This modification has been checked to have only a minor effect on the resulting microstructure, by comparing simulations of both wall morphologies, using vein perpendicular opening (Fig. 6).

A good agreement between the natural vein and simulations was found using isotropic growth of initial grains of approximately 35 μm width (Fig. 4c). The opening increment, which gave best results with 145 crack–seal events, is approximately 0.01 mm (reducing the increment below 0.01 mm has no effect). Growth competition takes place as a result of the rough wall geometry during the very early stages. During this phase, grain boundaries do not track the opening trajectory. Later, grain boundaries are stabilised at GBAs. From here on, crystal width is independent of the initial grain size and corresponds well with the observed fibre width.

3.3. Sensitivity analysis

In the subsequent sensitivity analysis, parameters were changed using the 'best case' simulation as starting point, varying one parameter at a time. Results of these are illustrated below.

3.3.1. Opening velocity

A decrease of the opening velocity (i.e. less crack events at constant crystal growth rate), leads to a vein very similar to the best case simulation. The vein is of course less wide after the same amount of time, but the width-to-length ratio of the crystals is constant and grain boundaries track the opening trajectory (Fig. 7a). Again grain boundaries are stabilised at GBAs. In contrast, *increasing* the opening velocity of the crack causes some grains to loose contact with the wall rock for several crack–seal increments. This partial sealing of the vein leads to partial tracking, i.e. grain boundaries do not track the opening trajectory continuously (Fig. 7c). The width-to-length ratio is not constant across the vein anymore and crystals become elongate-blocky. If none of the grains keeps contact to the wall rock, no grain boundary follows the opening trajectory (Fig. 7d).

In summary, a dramatic change of the crystal morphology and the tracking capability occurs, when the growth velocity is smaller or equals the opening velocity (Mügge, 1928; Urai et al., 1991). This transition is very rapid and takes place within a few per cent change in the opening velocity.

3.3.2. Initial grain size

Depending on the presence of nuclei in the wall, antitaxial calcite veins either start by epitaxial growth on these nuclei, or by nucleation in the zone which will later become the median line. A larger initial grain size results in wider crystals (Fig. 8). The position of the seed's grain boundaries relative to the GBAs determines their survival and the exact final vein morphology. This is illustrated on

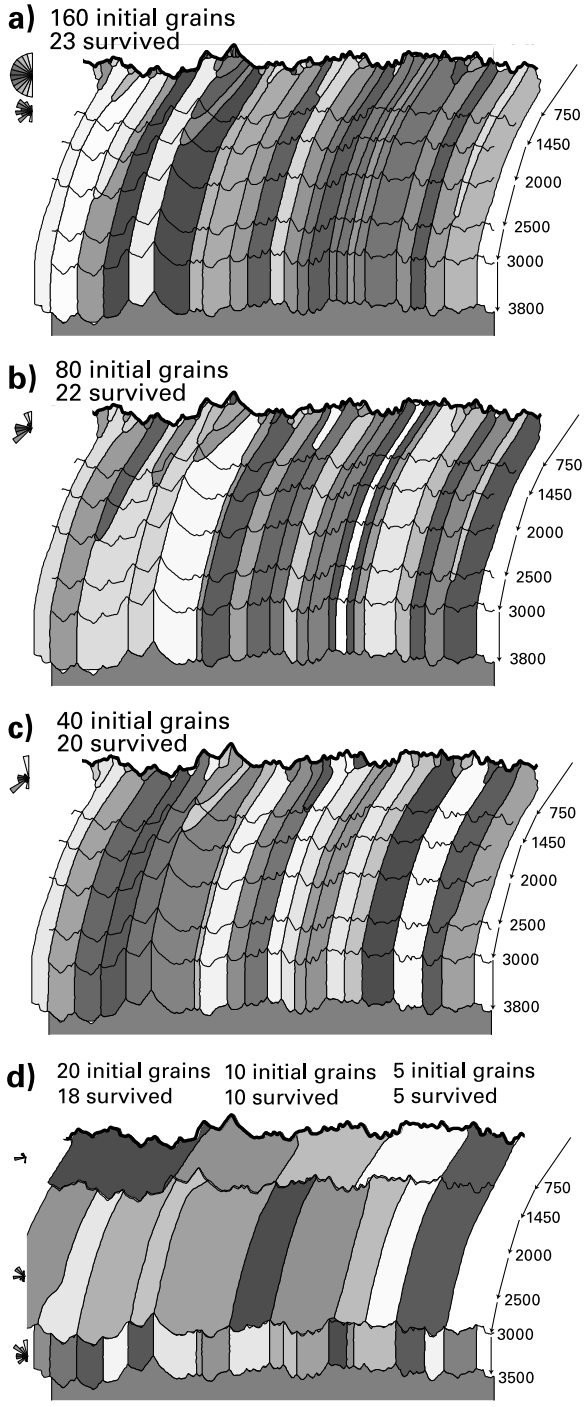

Fig. 8. (a) Simulations of different initial grain sizes. Decreasing the grain size does not lead to a significant change in fibre morphology. Grain boundaries are still located at antiformal peaks of the wall. (b) 'Best case' simulation. (c) An enlargement of the initial grain size leads to an increase in crystal width (right-hand side). An increase of the number of surviving grains on the left-hand sides indicates, that both the grain size and the position of initial grain boundaries is important for grain survival. (d) Overlay of 5, 10 and 20 initial grains. In all cases grain boundaries track the opening trajectory, independent of the initial grain size. While all grains survive, if few initial seeds exist (the case for 5 and 10 initial seeds), growth competition takes place for 20 initial grains.

the left-hand side of Fig. 8(c), where more grain boundaries are attached to GBAs as in the same region of Fig. 8(b), despite larger initial grains.

The tracking efficiency of grain boundaries is not influenced by the initial grain size. Boundaries between very large initial grains are also capable of tracking the opening trajectory (Fig. 8d; compare with the natural example in fig. 1g in Urai et al., 1991). Again all simulations show grain boundaries stabilised at GBAs.

In summary, both the tracking efficiency and fibrous morphology are unaffected by the initial grain size. Significant growth competition takes place only at the very early stages of crystal growth. If seed grain boundaries happen to be all located at GBAs, all initial grains will survive (Fig. 8d). A smaller initial grain size does not increase the number of surviving grains significantly.

3.3.3. Wall roughness

We investigated the effect of wall roughness by carrying out simulations using smoothed versions of the 'best case' wall geometry. Two series of simulations were carried out, one with progressive reduction of amplitude, and another with progressive removal of short-wavelength irregularities with a moving average filter.

For the amplitude reduction, the y-value of each point in the digitised wall was reduced by a constant factor. This results in less steep but equally frequent irregularities and finally a nearly flat wall (Fig. 9).

The amplitude reduction, somewhat surprisingly, leads to a decrease in final crystal width. Growth competition is suppressed due to the decrease of the number of GBAs, as shown in Fig. 9(d). Although grain boundaries are attracted to antiformal peaks (Fig. 9a–c), they are not stabilised there, and grain boundaries do not track the opening trajectory. The small grain boundary waves shown enlarged in the inset of Fig. 9(e) are each caused by a grain boundary losing contact with an imperfect GBA. At greatly reduced amplitudes, wall irregularities are insignificant and face controlled fibres develop.

Minor wall irregularities were removed using the moving average filter in the second series (Fig. 10), with filter width between 11 and 75 μm. This filter removes smaller undulations, but large peaks are preserved and remain relatively sharp. In these simulations the crystal width increases, and the tracking capability of grain boundaries remains constant.

In summary, the effect of smoothing the wall is that of decreasing the efficiency of GBAs (cf. figs. 6 and 7 of Urai et al., 1991). This results in marked changes in the resulting microstructure.

3.3.4. Growth anisotropy

A simulation of the natural vein morphology is also possible using anisotropic crystal growth with fastest growing facets normal to each other (that is spheres become cubes, see Bons, 2001). While Fig. 11(a) presents a simulation of fast growing anisotropic crystals, Fig. 11(e) uses the same

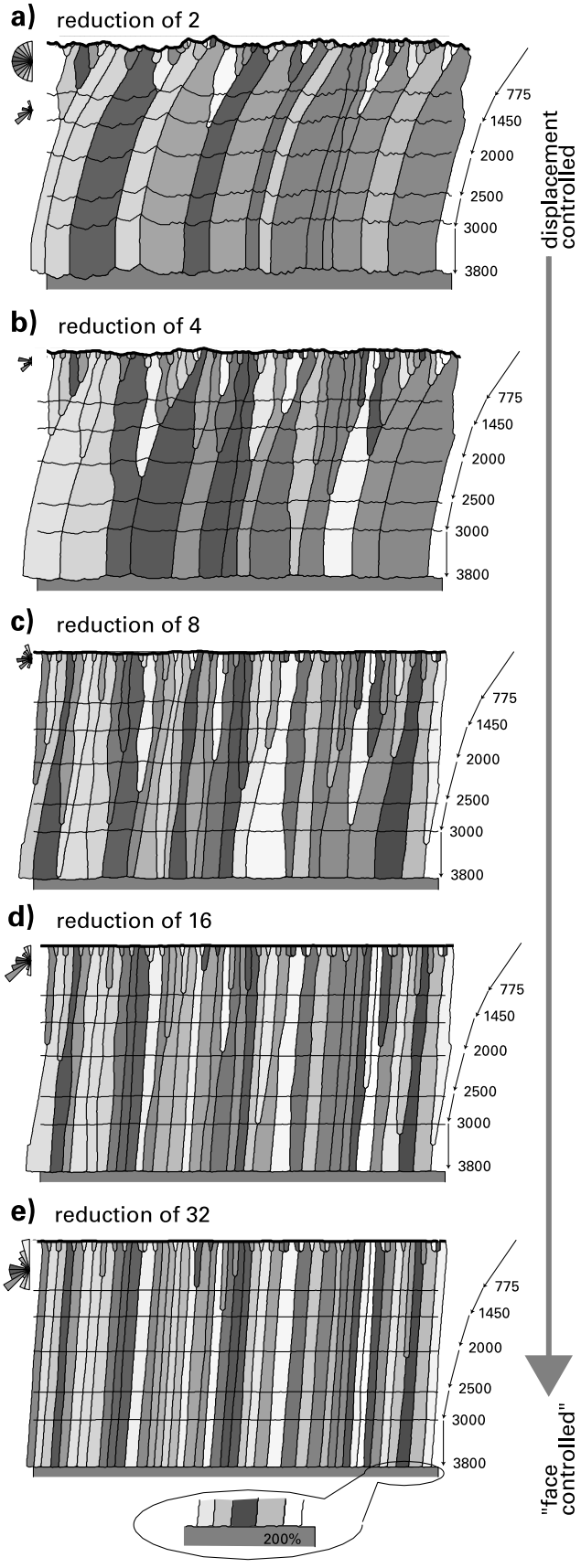

Fig. 9. Simulations of wall geometry deroughened by amplitude reduction. Reduction of the amplitude leads to the removal of the wall irregularities. Grain boundaries lose their tracking capability, although crystals keep their fibrous morphology and the number of surviving grains increases (b–e). Note that the angle between the flat wall and the fibres is not exactly 90°, but actually 86°. This is an artefact due to the way the early version of the program stored node data in memory. The resulting error only occurs in simulations of isotropic growth and a flat wall rock morphology.

opening trajectory, but the growth rate is smaller. A smaller growth rate leads to more anisotropic growth, the variation in crystallographic orientation is more limited. The tracking capability and fibrous morphology is unaffected. Similar to an increase of the opening velocity, a reduction in growth velocity leads to non-tracking grain boundaries with blocky morphology (Fig. 11b–d).

As explained in the introduction to the simulation (Fig. 3), growth competition (and the final crystal orientation distribution) is controlled by the wall morphology for isotropic growth. For anisotropic growth the final crystal morphology is also dependent on the grain orientation, but grain boundaries still track the opening trajectory if the crack is rough, the opening very narrow and the growth velocity equal to or larger than the opening velocity of the vein (Fig. 11a, e).

To further illustrate the role of growth anisotropy we ran two additional simulations in which the first half of the vein was grown in 'GBA control mode', followed by one very large opening step, after which the crystals grow as if in a free fluid. This leads to further growth competition in both cases, where in the isotropic case (Fig. 12a) faceting is not developed and in the anisotropic case (Fig. 12b) the crystals develop facets.

4. Discussion

The key microscale process which makes our simulations different from growth in a free fluid is the presence of the inert, rigid wall which forces the growing crystals to grow into a shape unrelated to their low-index crystallographic directions. This additional boundary condition, which is the cause of the formation of GBAs, has a major effect on the microstructural evolution, *if* it occurs *frequently enough*, i.e. the crack–seal increments are sufficiently small. Obviously this also requires that the crack is completely filled before the next opening event, i.e. the average opening velocity is equal to the velocity of the slowest growing crystal face. Fig. 13 illustrates how discontinuous and continuous accretion are end-members of a continuum, depending on the step size, with the corresponding effect on microstructure. As illustrated in Fig. 4, our simulations are capable of forming long, natural-looking fibres as long as the individual opening steps are not too large. On the other hand, decreasing the crack width below a critical value of 0.01 mm has no effect on the resulting microstructure. Therefore, as far as our

simulations are concerned, a discontinuous or continuous accretion process can both produce good fibres.

The key as yet untested assumption is that for very small crack–seal increments the kinematics of crystal growth in nature are similar to what is used in our model. One argument to support this is given by Urai et al. (1991), who suggest that the imprint of the wall makes the surface

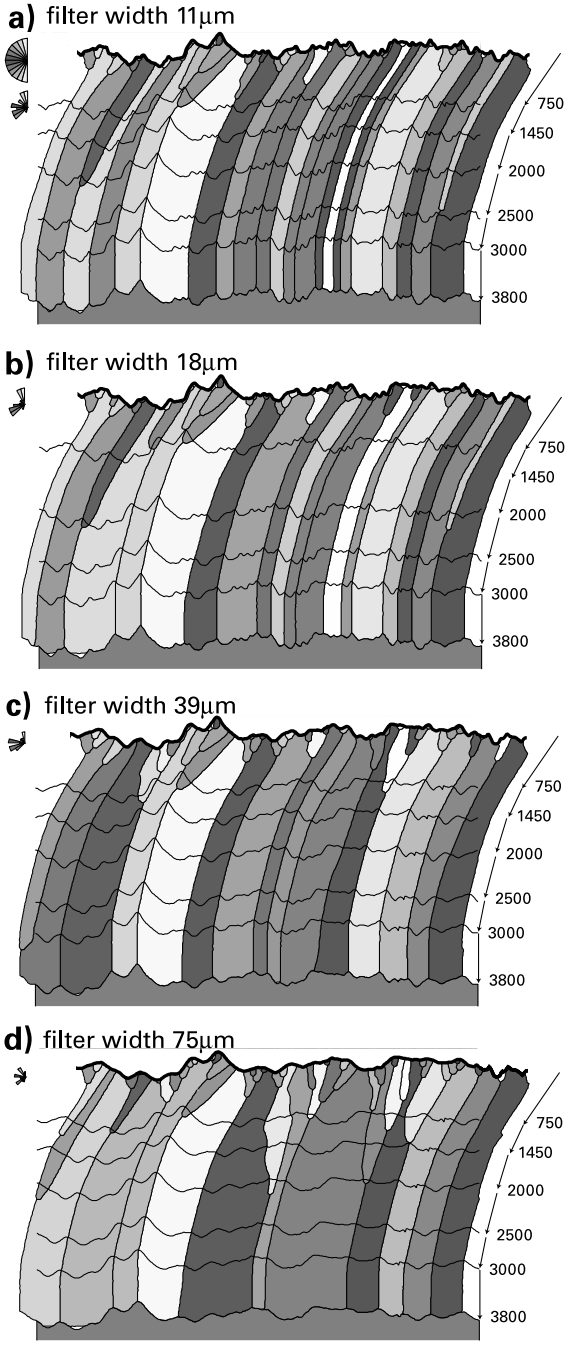

Fig. 10. Simulations of vein formation with the wall geometry deroughened by a moving average filter. The smoothening routine removes the minor peaks of the wall, which results in fewer surviving grains. The tracking capability is unaffected, grain boundaries are displacement controlled.

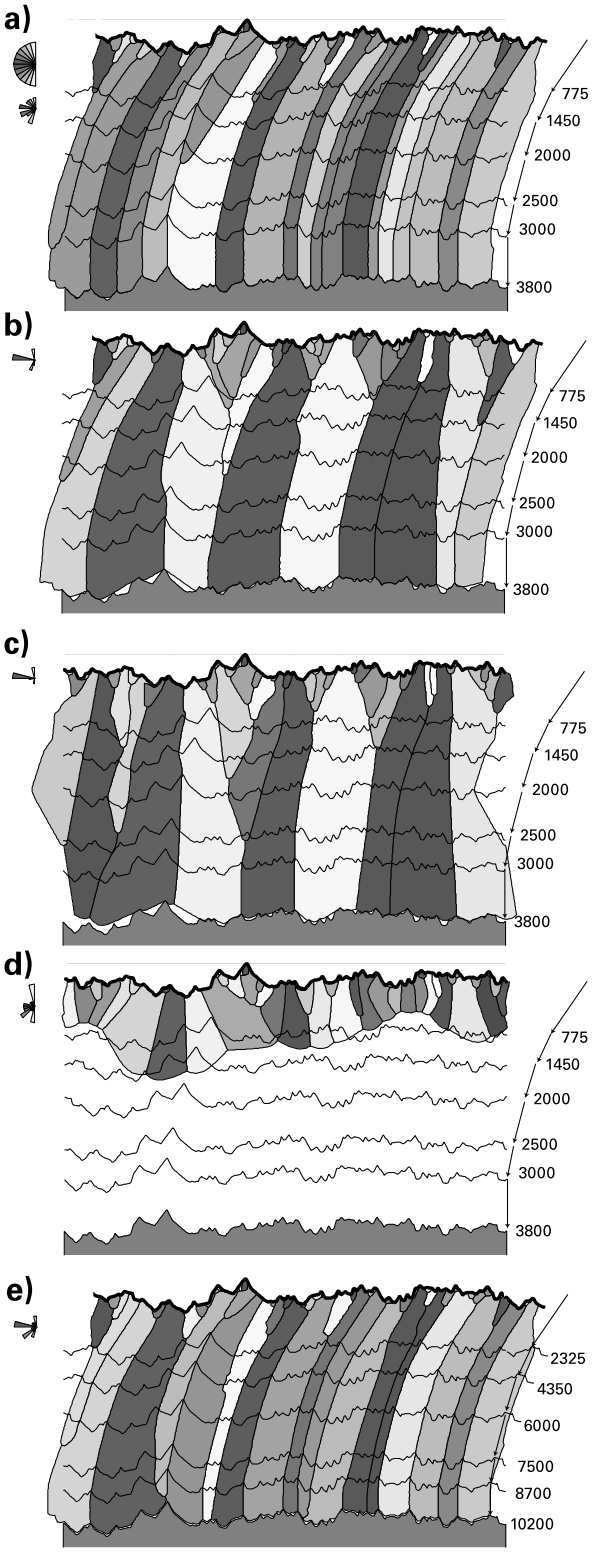

Fig. 11. Simulations of anisotropic growth show similar results as presented in Fig. 7, that is grain boundaries lose their tracking capability and grains become successively blocky, when the opening velocity is higher than the growth velocity (c, d). A reduction in crystal growth velocity and a simultaneously reduced opening velocity by the same factor shows that the vein remains fibrous (a, e).

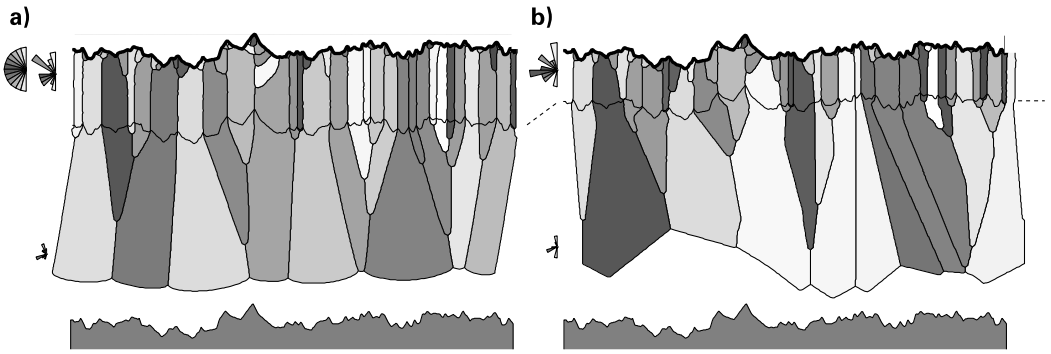

Fig. 12. (a) Fibrous texture of isotropic growing crystals changes to blocky texture at the outline of the wall within the vein. This is reached due to an increase of the opening increments, with the crystal growth rate smaller than the opening velocity. (b) Using anisotropic growth behaviour, again the texture changes from fibrous to blocky, but the polycrystal front is irregular.

temporarily 'rough' in the crystallographic sense, leading to isotropic growth kinetics of crystals which will develop facets after prolonged growth. The simulations presented here show that the strictly isotropic growth kinetics assumed in Urai et al. (1991) are not necessary for the simulations to work, and good fibres can be formed with anisotropic growth kinetics.

The next question, much more difficult to answer, is *how* wide the individual cracks can be before the development of facets starts to propagate the grain boundaries in directions not predicted in our models. Stated otherwise, what are the details of crystal growth on an irrational, e.g. fractured surface of a polycrystal? We know that after prolonged growth a microstructure dominated by low-index faces develops, but the key to the problem of syntectonic fibres is understanding the initial stages of the process during the accretion of the first few micrometres. As far as we know there is no information available on this topic. Further understanding of this is essential to assess the applicability of our simulations to nature.

One of the surprises of the SEM observations was that the vein walls cannot be identical to the initial fracture surface on which the vein started to grow. This indicates that the vein wall deforms during vein formation. We envisage two components of this deformation: one is due to deformation of the matrix which produces a lens-shaped vein out of an initially narrow crack. The other is due to breaking-off of wall rock fragments during opening of the crack, and the sealing of the crack by a hybrid process of unitaxial and bitaxial growth, as illustrated in Fig. 14. This process tends to locally enlarge the initial wall irregularities. We interpret part of the wall in the simulated vein to have developed by this process, and this interpretation is used to justify modification of the observed irregularities to the morphology used for our 'best case' simulation, which may represent the original shape of the wall.

Keeping the above arguments in mind, our best case simulation does produce a fibrous microstructure which is very similar to the one observed, using reasonable input parameters. Besides the shape of the crystals, the simulation also reproduces the observed fibre diameter, independently

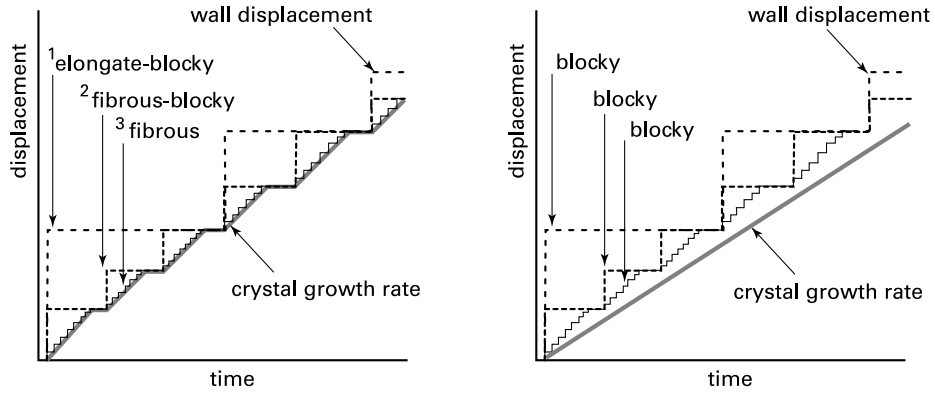

Fig. 13. Schematic illustration of the gradual transition between the discontinuous crack–seal process and continuous accretion. In the left-hand diagram the average velocity of crystal growth and crack opening is the same in all three cases, satisfying the Mügge (1928) requirement. In case 3 however, the number of times that the crystals and the wall are in contact is much larger, allowing better control of the wall on crystal morphology. With even smaller opening increments (nm scale), the process gradually becomes a continuous one. In the right-hand diagram the average velocity of crystal growth is less than the average opening rate, and the crystals effectively grow into a free fluid, producing blocky textures.

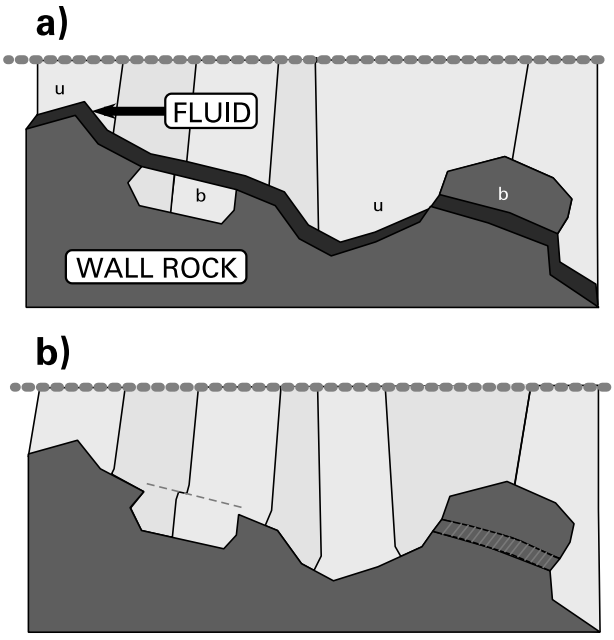

Fig. 14. Cartoon to illustrate the complications in microstructural evolution in a dominantly antitaxial vein, when the boundary crack follows the vein–wall boundary only partially. This is illustrated in (a) where on the left-hand side the crack locally intersects a grain of vein material, and on the right-hand side a bulge of the wall. Such structures are thought to evolve when the vein–wall interface has an 'interlocking' shape. u—unitaxial growth, b—bitaxial growth. Sealing of the crack is illustrated in (b), where the two 'exotic' portions of the crack are sealed by bitaxial growth, while the remaining portion is sealed by unitaxial accretion. Such processes are thought to be responsible for the very large wall rock irregularities.

of the initial grain size. We note however that the 'best case' simulation presented here is a possible, but non-unique solution (e.g. see Fig. 11a, e with anisotropic growth and similar good results).

On the other hand, we have also shown that by changing the input parameters to values which are also quite possible in nature, still natural looking but non-tracking fibres are produced. This again stresses the need in field studies to use every possible method to test the tracking hypothesis.

Finally it is worth commenting on the current discussion (Durney and Ramsay, 1973; Fisher and Brantley, 1992; Bons and Jessell, 1997) of microstructure versus transport mechanism, i.e. could fibres be diagnostic for growth in a stationary fluid with only diffusional transport? The model used in this study is purely kinematic, i.e. it does not incorporate the properties of the fluid between the vein and the wall. Considering the evolution of the space between the wall and the vein in our simulations, it is equally possible that the transport to the growing crystals is by diffusion, advection or a combination. Problems which have to be kept in mind are the sealing of the lateral transport path in our 2D simulations once one crystal touches the wall (this problem is much less important in a 3D situation) and the process of the final sealing of the crack (this probably occurs by a surface energy driven crack-healing stage, Lemmleyn and Kilya, 1960). Therefore, we argue that based on our results, both diffusion and advection are potentially capable of developing fibrous morphologies during unitaxial growth.

5. Conclusions

The growth and microstructural evolution of natural antitaxial fibrous veins can be successfully simulated, using observable properties and reasonable input parameters. Long axes of vein crystals have a potential to track the opening trajectory, if the wall rock is rough, the opening increments are small and crystals touch the wall before the next increment starts. The growth anisotropy and the initial grain size are of minor importance for the formation of fibrous veins. Growth competition is a natural consequence of the presence of the rough wall during unitaxial crystal growth. Crack–seal and continuous accretion are limits of a continuum, both can produce fibrous veins.

Acknowledgements

One of us (J.L.U.) wishes to acknowledge a series of stimulating and highly enjoyable discussions with Paul Williams and Win Means in the course of 1984, which started this project. Discussions with Paul Bennema opened new insight in the subject of crystal growth. Mark Jessell is thanked for help with the programming and many discussions about veins. Stephen Cox and Colleen Elliot reviewed the manuscript, and their contributions are gratefully acknowledged. We thank Werner Kraus and Wouter van der Zee for help with sample preparation and computer applications. This work was supported by grants of the Deutsche Forschungsgemeinschaft ur-98-1-1 to C.H., and pa-3-1 to D.K. P.D.B. acknowledges financial support through a Monash University Logan Research fellowship.

References

Bennema, P., 1996. On the crystallographic and statistical mechanical foundations of the forty-year old Hartman–Perdok theory. Journal of Crystal Growth 166, 17–28.

Bons, P.D., 1997. Crack–seal vein texture—a numerical model. Terra Nova 9 (Abstract suppl. 1), 172.

Bons, P.D., 2001. Development of crystal morphology during unitaxial growth in a progressively widening vein: I. The numerical model. Journal of Structural Geology 23, 865–872.

Bons, P.D., Jessell, M.W., 1997. Experimental simulation of the formation of fibrous veins by localised dissolution–precipitation creep. Mineralogical Magazine 61, 53–63.

Cox, S.F., 1987. Antitaxial crack–seal vein microstructures and their relationship to displacement paths. Journal of Structural Geology 9, 779–787.

Cox, S.F., Etheridge, M.A., 1983. Crack–seal fibre growth mechanisms and their significance in the development of oriented layer silicate microstructures. Tectonophysics 92, 147–170.

Crespi, J.M., Chan, Y.-C., 1996. Vein reactivation and complex vein intersection geometries in the Taconic Slate Belt. Journal of Structural Geology 18, 933–939.

Durney, D.W., 1972. Deformation history of the Western Helvetic nappes, Valais, Switzerland. Ph.D. thesis, London University.

Durney, D.W., Ramsay, J.G., 1973. Incremental strains measured by syntectonic crystal growth. In: de Jong, K.A., Scholten, R. (Eds.). Gravity and Tectonics. Wiley, New York, pp. 67–96.

Fisher, D.M., Brantley, S.L., 1992. Models of quartz overgrowth and vein formation: deformation and episodic fluid flow in an ancient subduction zone. Journal of Geophysical Research 97, 20043–20061.

Fisher, D.M., Brantley, S.L., Everett, M., Dzvonik, J., 1995. Cyclic fluid flow through a regionally extensive fracture network within the Kodiak accretionary prism. Journal of Geophysical Research 100, 12881–12894.

Hilgers, C., Urai, J.L., Post, A.D., Bons, P.D., 1997. Fibrous vein microstructure: experimental and numerical simulation. Aardkundige Mededelingen 8, 107–109.

Lemmleyn, G.G., Kilya, M.O., 1960. Distinctive features of the healing of a crack in a crystal under conditions of declining temperature. International Geology Review 2, 125–128.

Means, W.D., Li, T., 2001. A laboratory simulation of fibrous veins: some first observations. Journal of Structural Geology 23, 857–863.

Mügge, O., 1928. Über die Entstehung faseriger Minerale und ihrer Aggegrationssformen. Neues Jahrbuch für Mineralogie, Geologie und Paläontologie 58A, 303–348.

Passchier, C.W., Urai, J.L., 1988. Vorticity and strain analysis using Mohr diagrams. Journal of Structural Geology 23, 857–863.

Ramsay, J.G., 1980. The crack–seal mechanism of rock deformation. Nature 284, 135–139.

Ramsay, J.G., Huber, M., 1983. The Techniques of Modern Structural Geology. Volume 1: Strain Analysis. Academic Press, London.

Ramsay, J.G., Huber, M., 1987. The Techniques of Modern Structural Geology. Volume 2: Folds and Fractures. Academic Press, London.

Ramsay, J.G., Dietrich, D., Casey, M., 1982. Excursion A & B, Western Helvetic nappes. Field Guide International Conference on Planar and Linear Fabrics of Deformed Rocks, Zürich, Switzerland.

Simony, P.S., 1998. CTG Nuna Field Trip in honour of Paul F. Williams. Transect of the Rockie Mountain fold and thrust belt Canmore to Revelstoke. University of Calgary, Canada.

Spencer, S., 1991. The use of syntectonic fibres to determine strain estimates and deformation paths: an appraisal. Tectonophysics 194, 13–34.

Taber, S., 1918. The origin of veinlets in the Silurian and Devonian strata of central New York. Journal of Geology 26, 56–73.

Tang, C., Alexander, S., Bruinsma, R., 1990. Scaling theory for the growth of amorphous films. Physical Review Letters 64, 772–775.

Thijssen, J.M., Knops, H.J.F., Dammers, A.J., 1992. Dynamic scaling in polycrystalline growth. Physical Review B 45, 8650–8656.

Urai, J.L., Means, W.D., Lister, G.S., 1986. Dynamic recrystallisation of minerals. In: Hobbs, B.E., Heard, H.C. (Eds.). Mineral and Rock Deformation: Laboratory Studies—The Paterson Volume. Geophysical Monograph 36, pp. 161–199.

Urai, J.L., Williams, P.F., van Roermund, H.L.M., 1991. Kinematics of crystal growth in syntectonic fibrous veins. Journal of Structural Geology 13, 823–836.

Williams, P.F., Urai, J.L., 1989. Curved vein fibres: an alternative explanation. Tectonophysics 158, 311–333.